320707-F

THE UNIVERSITY OF MICHIGAN
COLLEGE OF ENGINEERING

Department of Aerospace Engineering
Gas Dynamics Laboratories

REDUCTION OF AERODYNAMIC DRAG ON TRUCKAWAY UNITS

D.R. Glass

Sponsored by the

NATIONAL AUTOMOBILE TRANSPORTERS ASSOCIATION

administered through

Department of Research and Development Administration
Ann Arbor

August 1978

ACKNOWLEDGMENTS

This work was done under contract with the National Automobile Transporters Association and was monitored by Mr. Douglas W. McGiveron, Executive Vice President and General Manager. Several members of that organization also participated in the planning of this wind tunnel test program.

The model of the 55 ft unit was provided by Traffic Transport Engineering, Inc. and the model of the 65 ft unit was provided by the Bankhead Transportation Co. The models were constructed by Mr. James R. Smith of Grosse Pointe Farms, Michigan. The automobile models were also molded by Mr. Smith, using a pattern model made by Julie A. Glass.

The author was assisted in this work by student research assistants, Nelson Orozco, Haider Sobh, James Van Lopik, and Roger Slykhouse as well as others on the Gas Dynamics Laboratories Staff.

SUMMARY

Wind tunnel tests have been made of models of a 55 ft truckaway unit and a 65 ft unit. The aerodynamic drag of such units when fully loaded is relatively high. At 55 mph the drag requires about half of the engine power output and about half of the fuel consumed is spent overcoming drag. Drag effects increase rapidly as the driving speed is increased.

The drag of truckaway units is greatly increased by cross winds. A 20 mph cross wind doubles the drag on a truckaway unit traveling at 55 mph.

The use of side panels (e.g. configuration 55-7-03 M4, see Appendices B and C) to reduce the cross flow through the loaded trucks can reduce the drag of the truck by about 20 to 30% for this relatively strong cross wind case. Fuel cost savings of about one cent per mile (based on current prices) appear possible for many operating conditions if appropriate side panels are used.

Various minor modifications can be made which would result in some reduction in the drag. On the 55 ft unit, for example, loading the headramp car so that it faces forward and is leveled (Config. 55-7-03 Baseline) reduced the overall drag by about 5% as compared to the headramp car facing backward and having its hood high (Config. 55-7-01 Baseline). On the 65 ft unit, turning the headramp car so that it faced forward and was level (Config. 65-8-02 Baseline) instead of facing backward and with the hood end low (Config. 65-8-01 Baseline) reduced the drag by over 2%. Further changes in the orientation might well produce some additional reductions in drag. Also, adding an insert ahead of the rear bulkhead on the 55 ft unit (Config. 55-7-03 M7C) reduced the drag by over 2%.

Modifications such as those listed above would result in modest savings in fuel, and other such minor improvements could be developed with more extensive testing, but the use of some sort of side panels would offer substantially greater savings than any other modification yet tested.

TABLE OF CONTENTS

LIST OF ILLUSTRATIONS

INTRODUCTION

A truck traveling at about 55 mph typically requires as much power to overcome aerodynamic drag as it does to overcome rolling friction. In other words, at "cruise" conditions about 1/2 of the fuel consumed is used to overcome air drag. At higher speeds the aerodynamic drag requires an even greater percentage of power and fuel.

With increasing fuel costs has come added incentive for reducing the aerodynamic drag of most automotive vehicles. New automobile designs are tested extensively in order to develop external configurations which will minimize air drag; busses are being reshaped to reduce the drag; and closed trucks are "sprouting" deflectors of various designs in an attempt to reduce the drag — and thereby reduce the fuel wasted.

Fully loaded truckaway units certainly have a very high drag at normal speeds. Considering the "aerodynamic" configuration of these vehicles, it seemed reasonable to expect that significant reductions in the drag forces would be possible. A series of wind tunnel model tests have therefore been made in an attempt to determine what could be done to reduce the drag of truckaway units, and the possible extent of such reductions.

This report presents the results of the wind tunnel tests of models of a 55 ft unit and a 65 ft unit. The more significant results and conclusions are included in the main body of this report. Additional detailed results and background information are included in the Appendices. It is intended that the main part of this report will be adequate for most purposes; the Appendices are included for the sake of completeness.

WIND TUNNEL TESTS

The two trucks under consideration here are a 55 ft long truckaway unit and a 65 ft truckaway unit. The frontal area of both of these vehicles is 8 ft by 13.5 ft or 108 sq ft. In order to conduct wind tunnel tests it was necessary to construct scale models of these two vehicles. The wind tunnel available for these tests at The University of Michigan has a test section which is 5 ft high and 7 ft wide. (See Appendix D for a description of this tunnel.) It is necessary that a model being tested in a tunnel not be too large relative to the tunnel size. It is also desirable that the model be as large as practical in order that the forces on the model will be reasonably large relative to the sensitivity of the tunnel's balance system. A model scale of 1 to 12 was selected as the optimum value for these tests. That is, the dimensions of the overall models, and each component of the models — insofar as practical, were 1/12 the corresponding dimensions of the full size trucks.

The equation used to relate the drag measured in the wind tunnel tests to the drag force on a full sized vehicle is the general drag equation:

$$F_D = C_D A(1/2\ \rho\ V_R^2) = C_D\ A\ q \qquad (1)$$

where

F_D = drag force, lbs

C_D = drag coefficient, determined primarily by the configuration of the vehicle

A = vehicle frontal area, sq ft

ρ = air density, lb/cu ft, divided by g, 32.17 ft/sec^2

V_R = relative air speed, ft/sec

$q = 1/2\ \rho\ V_R^2$ = dynamic pressure

The value of C_D, for a given body is largely determined by the shape of the body. In addition, the value of C_D will, in general, vary with the dimensionless parameter, Reynolds number, Re. (See Appendix A for the definition of Re and various other terms and equations.) However, for relatively bluff bodies, such as the truckaway units, the value of C_D may be relatively independent of the value of Re. These wind tunnel tests of

the truckaway models have shown that C_D is relatively unaffected by changes in Re, over the range of conditions tested. In view of this, the values of C_D determined during these wind tunnel tests can be used with reasonable confidence for the full scale trucks. It should also be noted that the value of C_D determined at one velocity can be used for a wide range of velocities to determine the drag force on a body, as per Eq. (1).

Since the full scale trucks are 12 times as wide and 12 times as high as the models tested, the frontal area of the truck is 144 times that of the model. Thus, for any given air speed, and assuming some standard air density, the measured drag on a model would be multiplied by 144 to determine the drag on a truck of the same configuration and at the same air velocity. However, it is much more useful to convert all test data into values of C_D; a wide range of full scale conditions can then be determined by use of Eq. (1). For this reason, all of the basic results of these wind tunnel tests will be presented in terms of the value of C_D. In addition, the effects of significant reductions in the value of C_D on the required engine horsepower and on the fuel costs will be discussed.

In order to measure the forces on a model in the wind tunnel it is necessary to support the model with a balance system which is capable of measuring the forces of interest on the model. The balance system used for these tests is described in Appendix D. Figure 1 is a photograph of the model of the 55 ft unit, loaded with 7 cars, mounted in the wind tunnel ready for testing. The flat surface just below the truck model is referred to as a ground board. This ground board is raised about 9 in. off of the tunnel floor. In this way the relative velocity of the air approaching the model is quite uniform, as it would be if a truck were traveling along a road in still air. If the model were at the level of the tunnel floor there would be a layer of low velocity (boundary layer) air near the floor of the tunnel which would result in incorrect drag force measurements.

It should be noted that while the model in Fig. 1 appears to be sitting on the ground board, it is actually not touching the ground board. Small posts pass through clearance holes in the ground board and connect some of the model's wheels to the balance system. These posts hold the model slightly above the ground board, so that forces on the model only are measured during the tests.

In order to present test results in terms of engine horsepower and fuel costs, certain equations and assumptions have been used. These are presented in Appendix A.

During these model tests over 40 different configurations were tested. Detailed descriptions of the various configurations tested are included in Appendix B. Detailed results of these model tests are presented in Appendix C. The more significant results are presented in the following section.

Figure 1 Model of the 55 ft Unit, Fully Loaded Mounted Above the Ground Board in the Wind Tunnel

TEST RESULTS

One of the first series of tests was made using the model of the 55 ft unit†, fully loaded. The value of C_D was found to be about 0.81, for the zero crosswind case. (See the tables in Appendix C for the various values of C_D referred to.) By applying this value of C_D to the full scale 55 ft truck traveling at 55 mph, assuming no wind, the following results are obtained:

Power needed to overcome rolling resistance	121 hp
Power needed to overcome aerodynamic drag	124 hp
Total power needed	245 hp
Fuel cost	12.2 ¢/mi

The equations and assumptions used in arriving at the above results are listed in Appendix A. While there may be some slight inaccuracies due to the assumptions made, the essential message is quite clear. At 55 mph the air drag requires about the same amount of engine power as does all of the rolling resistances. Also, aerodynamic drag is "eating up" half of the fuel being consumed!

The importance of air drag depends on the magnitude of the relative air speed, since drag is proportional to the square of the relative velocity. At very low driving speeds the power required to overcome drag is nearly negligible; at very high speeds the aerodynamic horsepower increases drastically, as shown by Fig. 2. The several curves of Fig. 2 show the effects of driving speed on;

1. engine power required to overcome rolling resistance, P_{e_R},
2. engine power required to overcome aerodynamic drag, P_{e_A},
3. total engine power, P_{e_T}, and
4. fuel costs per mile.

---

†For the sake of brievity the model of the 55 ft model will be referred to as the '55 ft model', although the actual length of the model is 55 inches. Similarily, the model of the 65 ft unit will be referred to as the '65 ft model'.

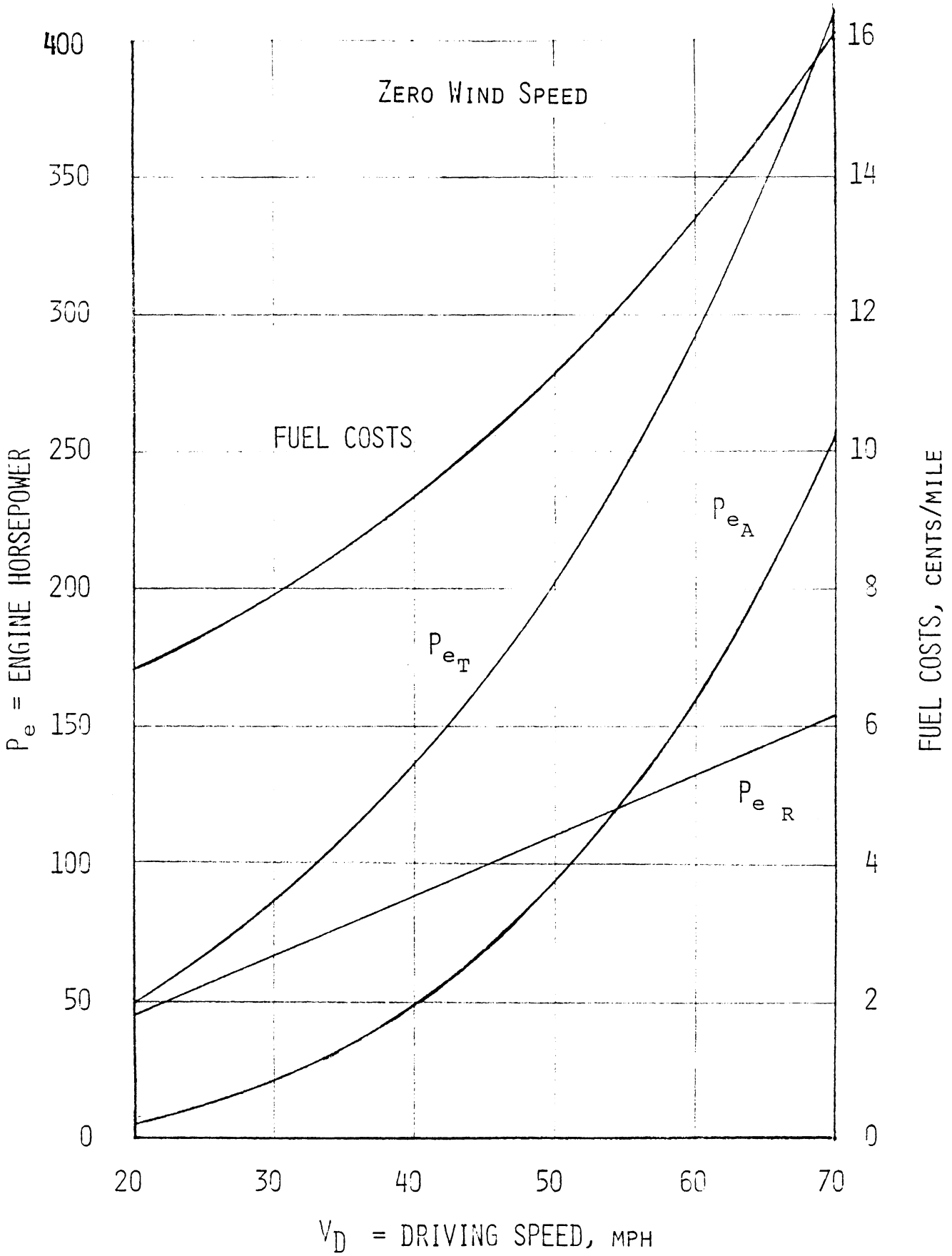

Figure 2 Effects of Driving Speed, 55 ft Unit, 7 Cars

The results of wind tunnel tests of the '65 ft model', fully loaded, have been used to produce similar curves for the 65 ft unit, see Fig. 3. As would be expected, the power required and the fuel costs per mile, at any given speed, are higher for the 65 ft unit than for the 55 ft unit. However, two general conclusions apply to both units:

1. Power and fuel consumption increase rapidly when driving speeds are increased.
2. At speeds of roughly 55 mph, about one half of the engine power and one half of the fuel used are required to overcome air drag. Therefore, any appreciable reduction in aerodynamic drag would immediately result in significant savings in operating cost. (Reductions in the drag coefficient are of even greater relative importance at higher speeds.)

The discussions thus far have been related to air drag on a truck for the no wind case. In this case the only air velocity relative to the truck, V_R, is due to the truck's velocity in still air. Here the magnitude of V_R is equal to the magnitude of the truck's driving speed, V_D. In general, however, there will be some wind velocity, V_W, which will be blowing at some angle, ϕ, relative to the vehicle's line of travel. Figure 4 shows the various velocity vectors and angles involved when there is a wind blowing. Note that in Fig. 4, V_R is shown as the resultant velocity; this resultant velocity is the velocity of the air relative to the vehicle. The angle between V_R and the vehicle axis is identified as ψ.

In wind tunnel tests the model can be rotated so that any chosen value of ψ is obtained. However, this does not determine the wind direction, ϕ, unless V_W and V_D are already fixed. In other words, a given value of ψ can correspond to many combinations of V_W and ϕ. In order to provide some "feeling" for the significance of ψ the following combinations are noted:

At $V_D = 55$ mph,
$\phi = 90°$ (i.e. a cross wind), and
$V_W = 20$ mph, then
$\psi = 19.98°$ or approximately 20°

At $V_D = 55$ mph
$\phi = 90°$, and
$V_W = 10$ mph, then
$\psi = 10.30°$ or approximately 10°

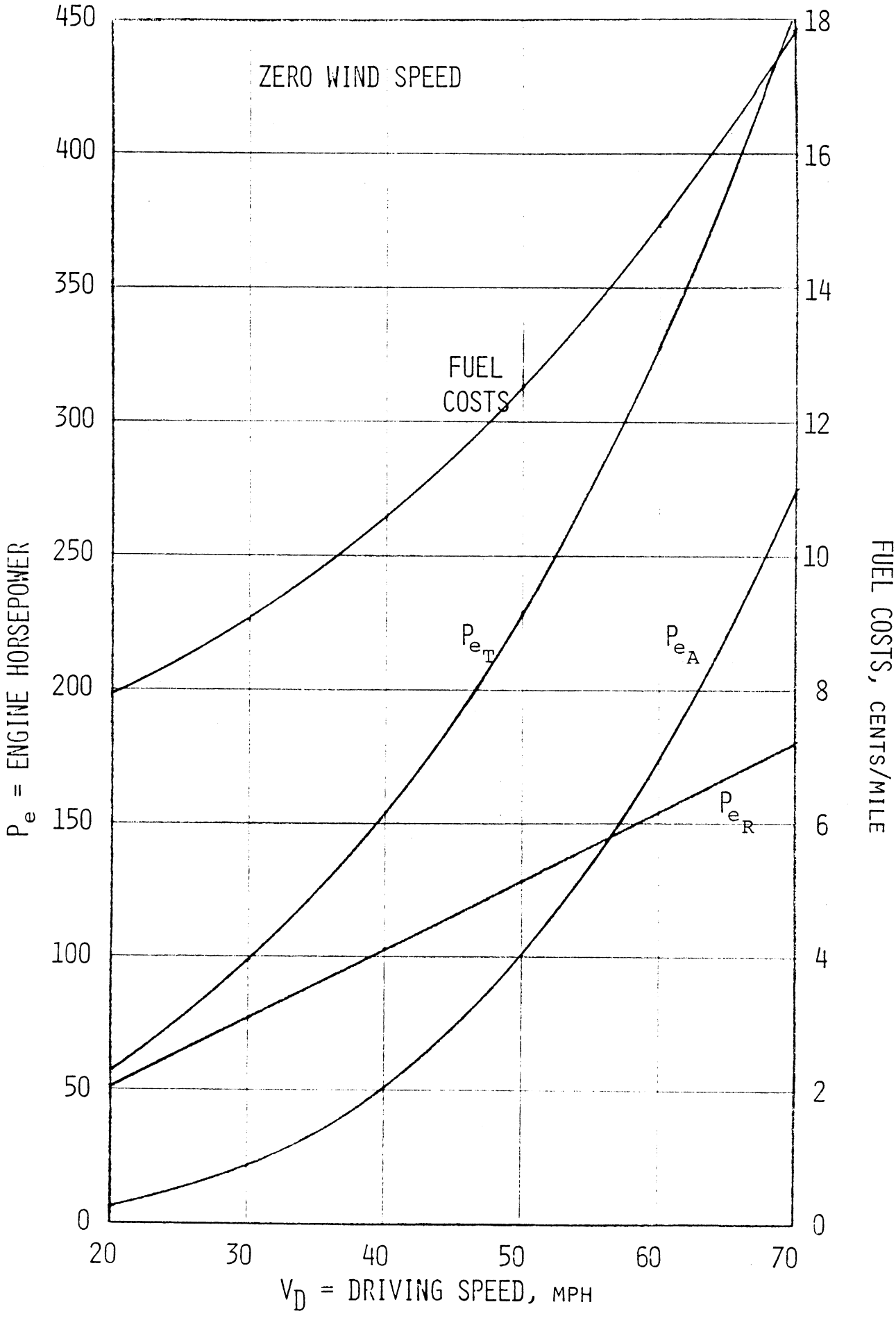

Figure 3 Effects of Driving Speed, 65 ft Unit, 8 Cars

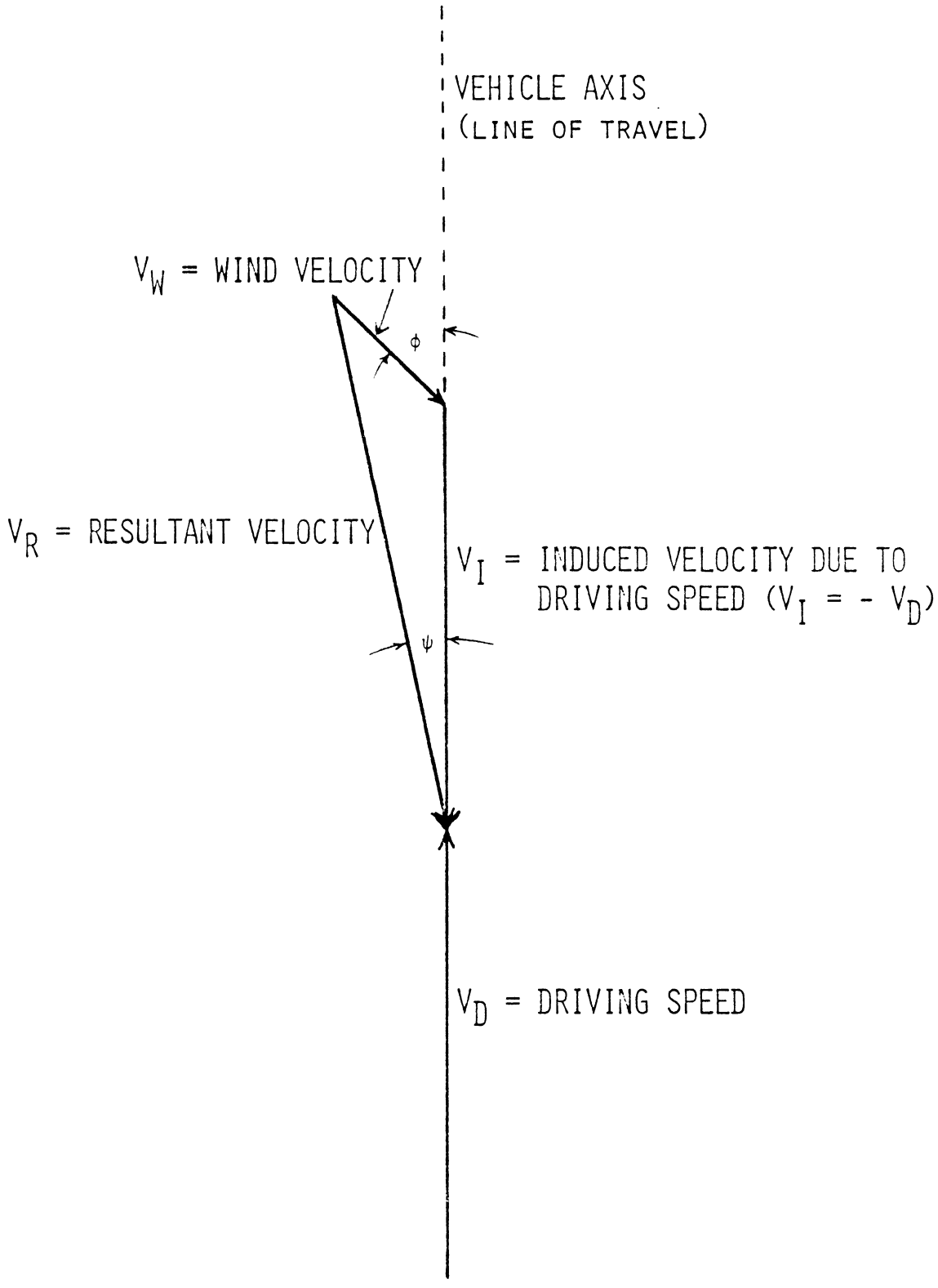

Figure 4 Diagram of Velocity Vectors Related to a Moving Vehicle

While a 20 mph cross wind is a relatively extreme case, certainly some cross wind can be expected so that in general ψ will not be equal to zero. Therefore these model tests have been made for various values of ψ from 0 to 20°. The results of "baseline" tests for the 55' and 65' models, both loaded and empty, are presented in Fig. 5 in the form of C_D versus ψ curves.

As Fig. 5 shows, the drag coefficient increases drastically with ψ. For example, with a driving speed of 55 mph and a 20 mph cross wind (i.e. ψ = 20°) the drag of each truckaway unit (55'and 65') is more than double the no-wind drag case. (It seems unlikely that most trucks would have the power to maintain a 55 mph speed with a 20 mph cross wind.)

Most vehicles have a higher drag when there is a cross wind, but these truckaway units are particularly bad in this respect. Because of this excessively high drag in a cross wind it was decided that further wind tunnel testing should concentrate on those configurations which reduced the drag coefficient significantly when there was a cross wind. Consequently, most further tests were made at ψ = 20°.

The basic purpose of these wind tunnel tests was to determine how the drag of the truckaway units could be reduced, and how much reduction could be expected. It was therefore planned that a wide variety of modifications would be made and tested. These modifications were to include various baffles, deflectors, the rounding of certain surfaces and different orientations of the automobiles loaded on the truck.

The modification which produced the most dramatic reduction of drag was the addition of side panels on the truck. Side panels generally reduced the drag by about 20 to 30%, depending on the truck model and the panel arrangement, for the case where ψ = 20°. No other modification resulted in nearly so great a reduction in drag.

In order to demonstrate why the side panels are so effective in reducing the drag, a few tests were made using smoke injected into the tunnel airflow so that the flow around the truck could be "seen". Figure 6 includes photographs of two such tests. In these tests the camera was mounted above the tunnel looking down on the top of the truck model (the 55 ft unit in this case). The front of the truck is to the left and the air flow is from the left to the right; the flow is at 20° to the truck axis (ψ = 20°). The smoke is injected upstream of the truck at a height of roughly 6 in. (This corresponds to a 6 ft height on the full scale truck.)

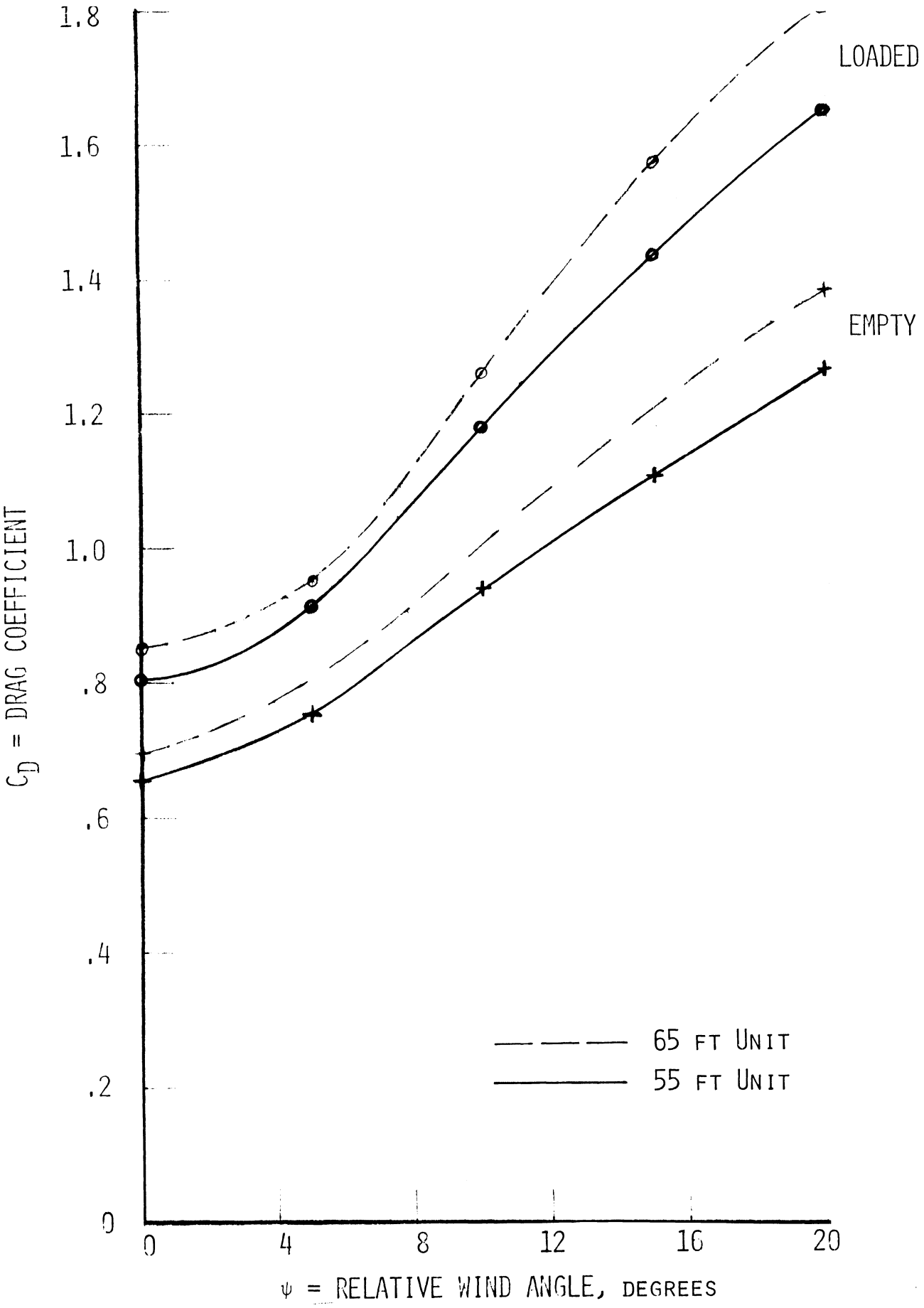

Figure 5 Drag Coefficient of Loaded and Empty Trucks

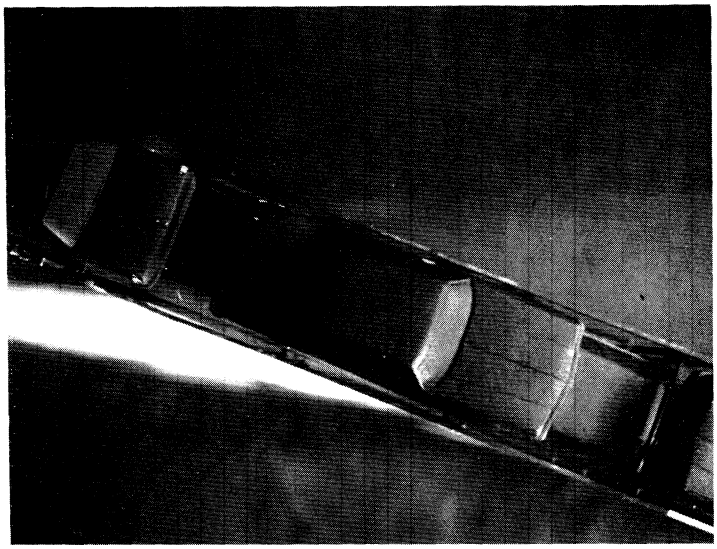

Model Configuration
55-7-03 - Baseline

(No Modifications)

Relative Air Velocity
(Front of truck is at left)

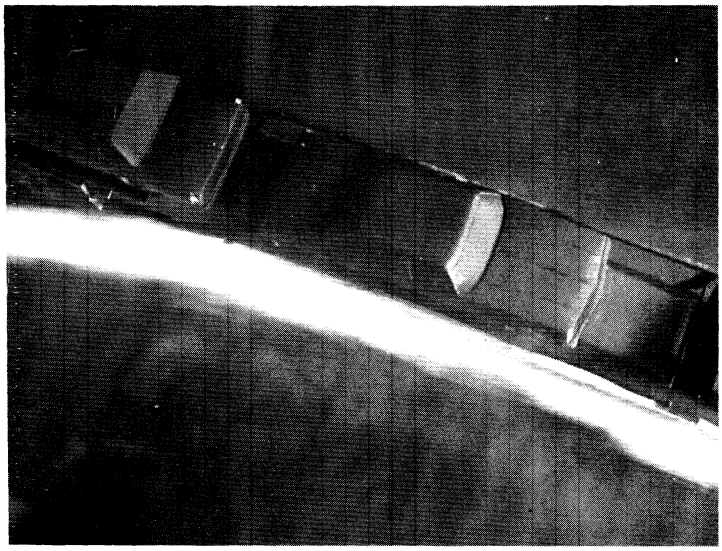

Model Configuration
55-7-03 - M4L

(Side Panels on
Left, Upwind Side)

Figure 6. Photographs of the airflow patterns through and around a fully loaded auto carrier. The relative wind is at 20° to the longitudinal axis of the truck.

In the upper picture of Fig. 6 the model is in the baseline configuration, i.e. no modifications have been made. Clearly the air approaching the truck, which is made visible by the smoke, flows right in among the cars. Although it is not so clearly visible in this photograph, the flow (smoke) was observed to be coming out on the opposite side of the truck. The turbulence generated by the air flowing around the cars is evidenced by the fact that the smoke stream has been broken up and dispersed.

The situation is entirely different in the lower picture of Fig. 6. Here the left side[†] has been covered by a solid panel. Now the oncoming air is gently deflected downwind, as shown by the smoke stream along the side of the truck.

In the first case (the upper photo of Fig. 6) the air flowing in among the cars is greatly slowed down, thus producing a considerable increase in drag. (In real life the air flowing in among the cars is actually accelerated, and to some extent carried along with the truck, thereby resulting in increased drag.) These tests and the various drag measurement tests have led to the conclusion that the key to reducing drag, for the cases where 4 is greater than zero, is the reduction of cross flow among the cars. Thus far, side panels have been the most effective way found to reduce the cross flow.

In order to demonstrate the potential savings in engine horsepower and fuel consumption which could result from the use of side panels, a series of performance calculations have been made. The equations and assumptions used to make these calculations are listed in Appendix A. The basic drag coefficient data used are included in Appendix C. In making these calculations a fully loaded 55 ft unit was considered. It was also assumed that the truck was traveling at a driving speed of 55 mph on a level road and that there was a 10 mph wind blowing. The full range of wind directions of from 0° (a head wind) to 180° (a tail wind) was considered and the results are plotted against wind direction in Fig. 7.

[†]The left side is the upwind side for these pictures, in most other tests discussed in this report, the right side is the upwind side.

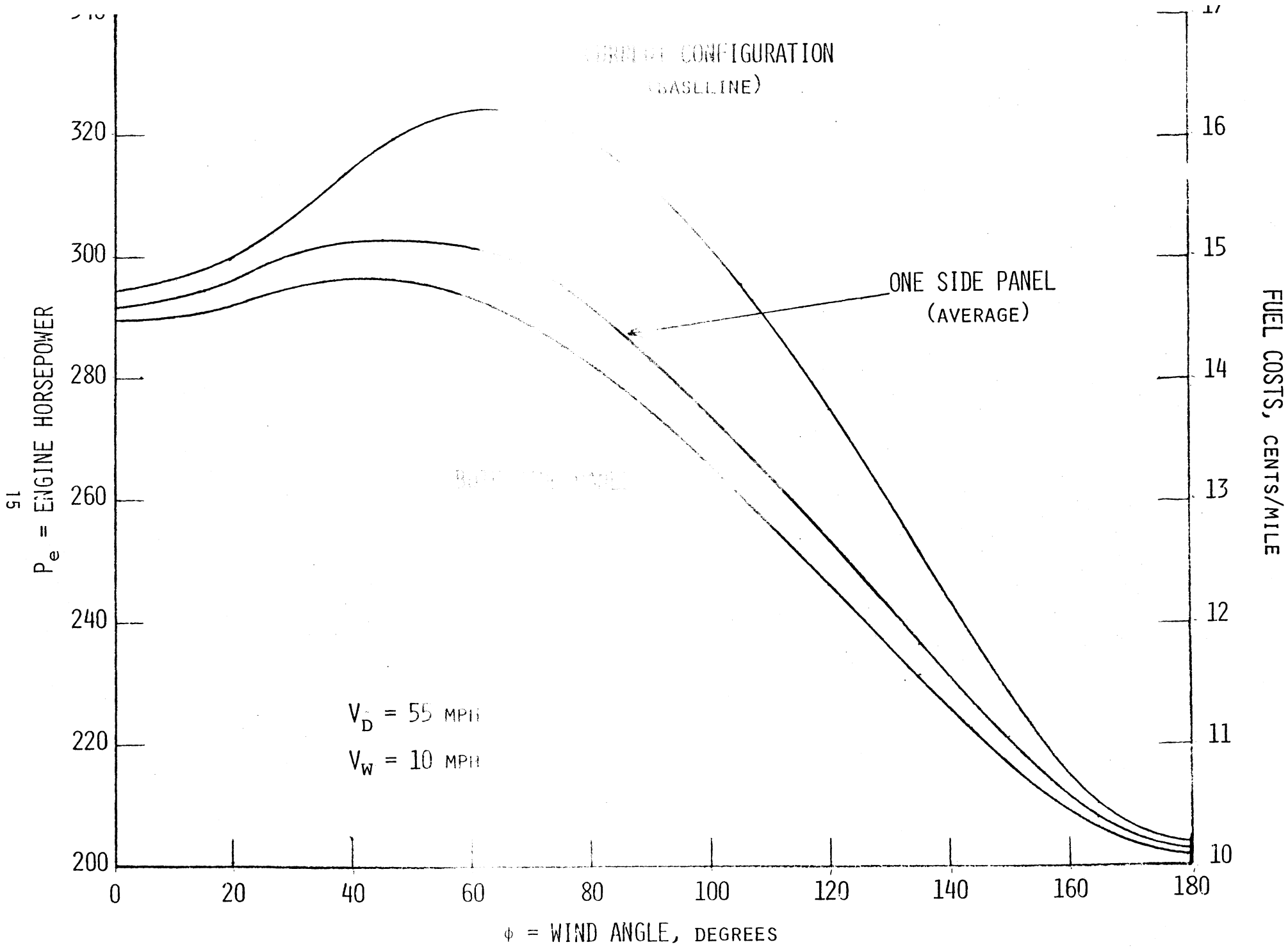

Figure 7. Engine Horsepower and Fuel Costs Versus Wind Angle, for a Loaded 55 ft Unit

The top curve of Fig. 7 indicates the engine horsepower needed and the resulting fuel consumption for the standard, or baseline, fully loaded configuration, over the full range of wind directions. The lower curve shows the corresponding information for the loaded case when full side panels are added. The intermediate curve represents the performance when only one side panel is installed. However, for this single side panel case, the average between the C_D for the case when the panel was on the upwind side and the C_D for the case when the panel was on the downwind side was used. This seemed to be the best way to evaluate the overall advantage of a single side panel in actual operation.

As noted earlier, the side panels are of the most benefit when the wind is primarily from the side. In normal operation the wind would be expected to range between 0 and $\pm$ 180°, so some average benefit would result. However, Fig. 7 shows that for most wind directions, over one cent per mile would be saved by the use of both side panels. Note that this is for only a 10 mph wind. The savings would be appreciably more at higher wind speeds.

In order to determine the saving more accurately, it would be necessary to assemble and incorporate statistical data regarding the local wind level and direction relative to a given truck route. This additional study is beyond the scope of the present research program.

As noted before, the side panels were found to be the most effective way to reduce drag for the cross wind cases. They were not quite as effective in reducing the drag on the 65 ft unit as they were in reducing the drag on the 55 ft model. (See specific results listed in Appendix C.) Therefore, if a set of curves, similar to those of Fig. 7, were prepared for the 65 ft unit the savings would be somewhat less, but they would still be quite significant; nearly one cent per mile saving should be possible for most wind directions.

Many modifications which were less drastic than adding side panels were tested. Several of these reduced the drag (at ψ = 20°) by a few percent. The various modifications tested are identified in Appendix B; the results are tabulated in Appendix C. A few of these more important modifications are also noted here briefly (for ψ = 20°):

1. The orientation of the cars makes some difference. For the 55 ft unit, orientation 1 had 5.4% more drag than orientation 3 (see Appendix B for description of orientations and configurations).

2. A bottom panel under the trailer of the 55 ft unit increased the drag by almost 2%. However, when the bottom panel was installed in addition to the side panels, the bottom panel reduced the drag by an additional 1%, roughly, over the side panels alone.

3. A fairing added behind the cab increased the drag. However, when the fairing was added to the side panels, on the 65 ft model, the drag was reduced by an additional 5% over the reduction due to the side panels only.

4. Adding porous panels (about 12% open) to the sides of the 65 ft model reduced the drag (at $\psi = 20°$) by only 6.1% while the solid side panels reduced the drag by 17.8%. (Side panels plus cab fairing reduced drag by 22.8%.)

Much of the effort during these wind tunnel tests has been directed toward the finding of ways to significantly reduce the aerodynamic drag. The results have shown that some form of side panels would significantly reduce the drag and provide appreciable savings in fuel costs.

With much more extensive testing of a great many small changes, the drag could probably be reduced by a few percent "here and there" so that a net reduction of several percent (e.g. 10 to 20%) might be achieved, even without the use of side panels. However, the results of tests made thus far have shown that panels, or some such device, which greatly reduces the cross flow of air through the loaded truck are by far the most effective way to achieve significant reductions in drag.

APPENDIX A
EQUATIONS AND ASSUMPTIONS

Several basic equations have been used in the interpretation and presentation of the results of this wind tunnel study. Also, in order to relate the drag measurements to fuel consumption and costs certain assumptions have been made. These equations and assumptions are listed here.

As noted earlier, the general drag equation is:

$$F_D = C_D\, A(1/2\ \rho\ V_R^2) = C_D\, A\, q \qquad (A.1)$$

where

F_D = aerodynamic drag force, lbs
C_D = coefficient of drag
A = frontal area, sq ft
ρ = air density, lb/cu ft divided by g, 32.17 ft/sec^2
V_R = relative air velocity, ft/sec
$q = 1/2\ \rho\ V_R^2$ = dynamic pressure (or velocity head)

The force required to overcome rolling resistance, which includes bearing forces as well as rolling forces on the tires, is usually approximated by the simple equation:

$$F_R = C_R\, W_{GV} \qquad (A.2)$$

where

F_R = rolling resistance, lb
C_R = coefficient of rolling resistance, lb/lb of W_{GV}
W_{GV} = gross vehicle weight, lbs

The total force, F_T, required to keep a vehicle moving at a constant speed on a level surface is simply:

$$F_T = F_D + F_R \qquad (A.3)$$

Obviously the force required to accelerate the vehicle and the force required to climb a hill would be added to the force determined by Eq. (A.3). All discussions which follow deal only with trucks traveling at constant speed on a level surface.

The actual engine power required to keep a truck moving is determined by the equation:

$$P_e = 1/\eta \; F_T \; V_D/550 \qquad (A.4)$$

where

P_e = engine power output, HP

η = ratio of the power delivered to the wheels to the engine power output. (Usually referred to as the power transfer efficiency.)

V_D = driving speed, ft/sec

In application the velocities will be expressed in miles per hour rather than ft/sec. The above equations will be adjusted accordingly.

In order to demonstrate the effects of drag reductions on engine power requirements it is necessary to make several assumptions. While the values assumed here cannot be equally accurate for all trucks and conditions, they should be suitable for the present purposes. These assumptions are:

η = 0.80

C_R = 0.011

ρ = "standard" air density = $(0.0765 \text{ lb/ft}^3)/(32.17 \text{ ft/sec}^2)$

SFC = 0.39 lb/HP hr (engine specific fuel consumption)

Fuel Price = \$.50 per gal

Fuel Weight = 7.12 lb/gal

A = 108 ft^2 (for 55 ft and 65 ft units)

W_{GV} = 60,000 lb for 55 ft units

= 70,000 lb for 65 ft units

Combining the above equations:

$$P_e = 1/\eta \; (C_D \; A \; 1/2 \; \rho \; V_R^2 + C_R \; W_{GV}) \; V_D/550 \qquad (A.5)$$

For the 55 ft unit at 60,000 lb, Eq. (A.5) becomes:

$$P_e = (C_D \; V_R^2/1086 + 2.2) \; V_D \qquad (A.6)$$

For the 65 ft unit at 70,000 lb, the corresponding equation is:

$$P_e = (C_D \; V_R^2/1086 + 2.57) \; V_D \qquad (A.7)$$

The cost of diesel fuel per mile is computed by the equation:

$$\text{Cost/Mile} = (\text{SFC} \times P_e/V_D)\ \text{Fuel Price/Fuel Weight} \qquad \text{(A.8)}$$

For the 55 ft unit:

$$\text{Fuel Cost/Mile} = 2.74\ (C_D\ V_R^2/1086 + 2.2),\ \text{Cents/Mile} \qquad \text{(A.9)}$$

For the 65 ft unit:

$$\text{Fuel Cost/Mile} = 2.74\ (C_D\ V_R^2/1086 + 2.57),\ \text{Cents/Mile} \qquad \text{(A.10)}$$

In Eqs. (A.6) through (A.10), the velocities are in mph. It should also be noted that V_R, the relative air velocity, and V_D, the driving speed, are the same only where there is no wind blowing.

In many fluid dynamic problems the dimensionless parameter Reynolds number, Re, is an important variable. Reynolds number is defined by the equations:

$$\text{Re} = \rho V \ell/\mu$$

ρ = fluid density

V = velocity

ℓ = a characteristic length

μ = fluid viscosity

This parameter represents the ratio of inertia forces to the viscous forces, in the fluid. For dynamic similarity to exist between two different conditions the value of Re should be the same for both conditions. This is especially true for streamlined bodies, such as airplane wings, etc., and for well rounded shapes such as spheres and cylinders. However, for bluff bodies and bodies with sharp corners the character of the flow around the body may be quite similar for a wide range of Reynolds number; in such cases the resulting drag coefficient will also be independent of Reynolds number, over a wide range of Re.

In this study to determine the aerodynamic drag on trucks, based on model tests, the air density and the air viscosity can both be considered relatively constant. Thus, in order to have the value of Re the same for the model tests as for the full scale truck operating conditions:

$$V_M \ell_M = V_{FS} \ell_{FS}$$

But the model length is 1/12 that of the full scale truck. The model velocity would then have to be 12 times that of the full scale truck in order to match the full scale Reynolds number. Obviously it is not practical to make wind tunnel tests at, for example, 12 x 55 mph. Therefore, we are forced to make wind tunnel model tests at lower values of Reynolds number than would ideally be desirable. However, since the trucks in question are relatively bluff bodies, with many relatively sharp corners, there is good reason to expect that the values of the drag coefficient would be largely independent of Reynolds number. During these wind tunnel tests the value of Re was varied by varying the air speed from about 40 mph to over 120 mph. The test results indicated very little variation of C_D with Re; in most cases there was no consistent variation of C_D with Re. It was therefore concluded that the values of C_D determined by these wind tunnel tests can be used with reasonable confidence for calculating the drag of the full scale trucks.

APPENDIX B
CONFIGURATIONS OF TRUCKAWAY MODELS TESTED

NUMBERING SYSTEM

The numbering system was set up to identify the corresponding full scale length of the model being tested, the number of automobiles on the truck, the orientation of the cars, and the modification (if any) made to reduce the drag. For example, configuration number 55-7-01-M5 stands for a 55 ft unit with 7 cars, loaded with automobile Orientation 1, and with Modification number 5. The various other configurations tested will be identified in the list of configurations that follows. In most cases a picture is presented which corresponds to each configuration listed. Since these pictures were meant to call attention to those particular features which were significant for that configuration, they do not always provide a good view of the overall model.

Table B-I lists the various configurations of the model of the 55 ft unit which were tested; Table B-II lists those configurations of the model of the 65 ft unit tested. Since the test results of the 55 ft unit model were already available when the tests of the 65 ft unit model started, it was not necessary to test many of those modifications which had proven to be of little or no benefit in reducing the drag on the 55 ft unit. However, other modifications, such as the porous side panels, were included in the tests of the 65 ft unit.

TABLE B-I CONFIGURATIONS TESTED - 55 FT UNIT

(Photographs are Shown in Fig. B-I)

Configuration No. 55-	
7-01 Baseline Photo A	The 55 ft unit, with the 7 cars having orientation number 1. The orientation of the 7 cars was the same for all tests made with the truck loaded, except for the headramp car. In orientation 1, the headramp car is loaded facing backward and with its hood end high. The Baseline configuration means that no "drag reduction" devices have been added.
7-02 Baseline Photo B	Same as 7-01 Baseline, except that the headramp car has been leveled as much as possible (orientation 2).
7-03 Baseline Photo C	The headramp car is facing forward and leveled as much as possible (orientation 3). Note: It was felt that this configuration was the most nearly "typical" of a 55 ft unit loaded with 7 automobiles. Therefore, all other test results are compared to the results of tests of configuration 7-03 Baseline, unless specifically stated otherwise.
7-03 M1 No Photo	Complete panel under bottom of trailer unit.
7-01 M2 Photo D	The front bumper is extended almost to the ground.
7-03 M3A Photo E	Selected side panels on trailer; rear panel section left off both sides.
7-01 M4† Photo F	Full side panels on both sides. In this picture the truck is yawed to 20° and only the panels on the right side — the upwind side in this case — can be seen; the paneling on the left or downwind side is the same as on the right side.
7-03 M4R† Photo G	Full side panel on right (upwind) side only.
7-03 M4L† No Photo	Full side panel on left (downwind) side only.
7-03 M5 No photo	Front bulkhead of trailer removed.

†Plus M1 - Bottom panel added to make an additional configuration.

TABLE B-I (concluded)

Configuration No. 55-	
7-01 M6 Photo H	Fairing, from cab to posts behind cab and to the bar above the cab.
7-03 M7 Photo I	Area between cars (i.e. between the downwind end of one car and the upwind end of the next car) filled in with foam. Also, the triangular solid region just upstream of the rear wheels of the trailer is filled in.
7-03 M4L + M7 Photo J	Full left panel plus fill in between cars and at bulkheads at both ends of the trailer.
7-03 M4L + M7A No Photo	Full left panel plus 3 bottom inserts between cars (2 inserts between cars plus the triangular insert at the rear of the trailer).
7-03 M7B No Photo	Three bottom inserts only.
7-03 M7C Photo K	Triangular insert at bottom rear of trailer only.
7-03 M7D Photo L	Triangular insert at bottom rear of trailer only. Larger and smoother than M7C.
7-03 M7E Photo M	Triangular insert plus fill in between cars.
7-03 M7F Photo N	Triangular insert plus fill in between cars plus fill in between bulkhead and front lower car.
7-03 M7F + M3R Photo O	Fill in between cars and right (upwind) side of cars "covered".
7-03 M7F + M3R + M1 No Photo	Fill in between cars, cover over right (upwind) side of cars and bottom panel added.
Empty Baseline Photo P	Empty trailer, baseline conditions

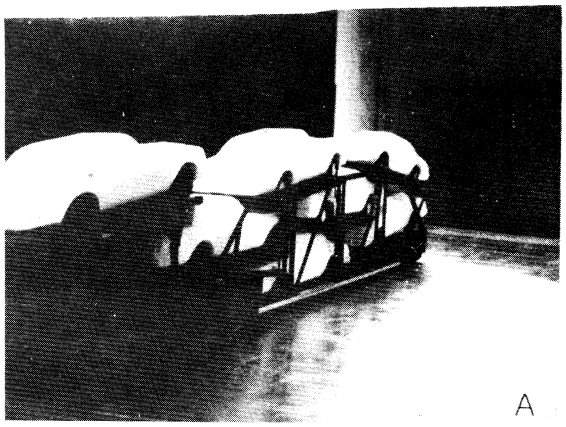

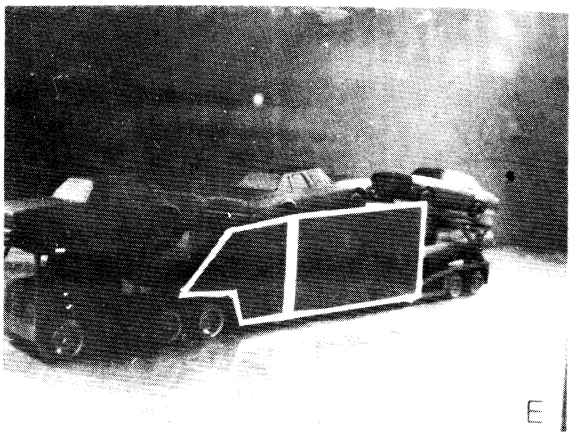

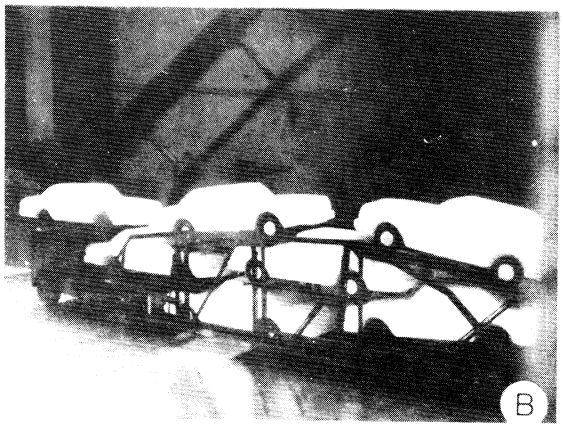

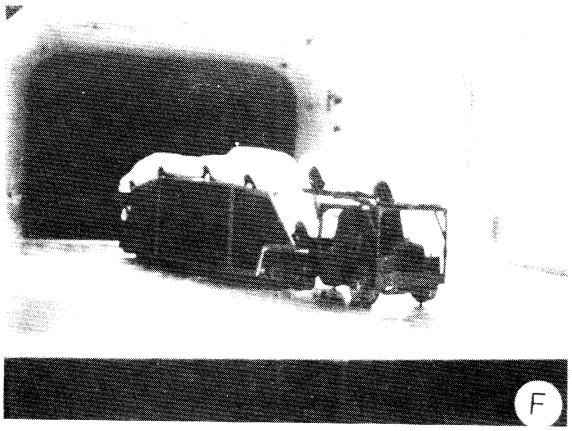

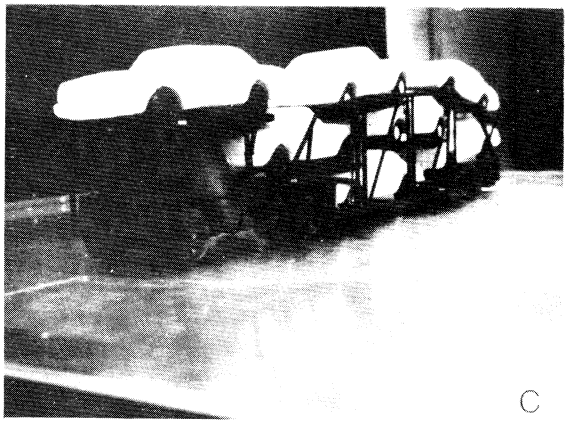

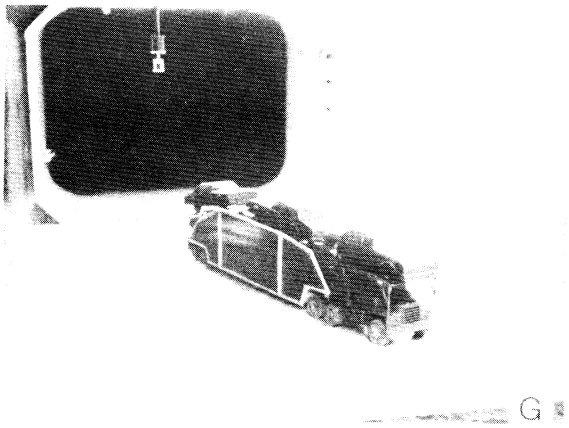

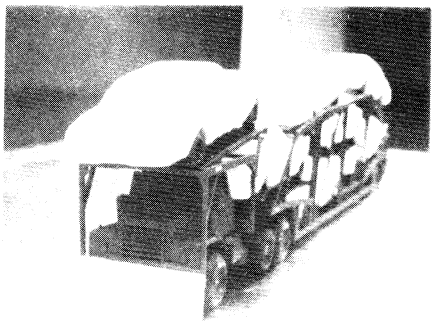

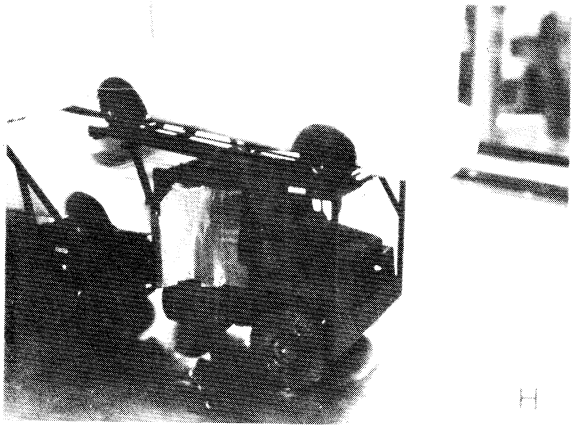

Figure B.1. Photographs of Model Configurations Tested - 55 ft Unit

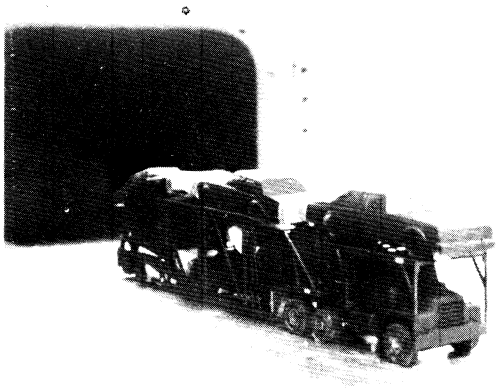

I

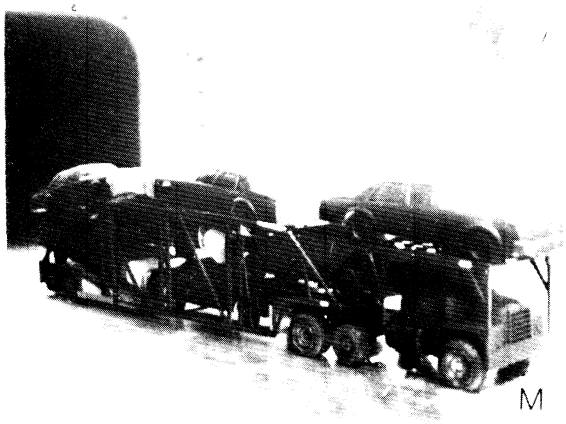

M

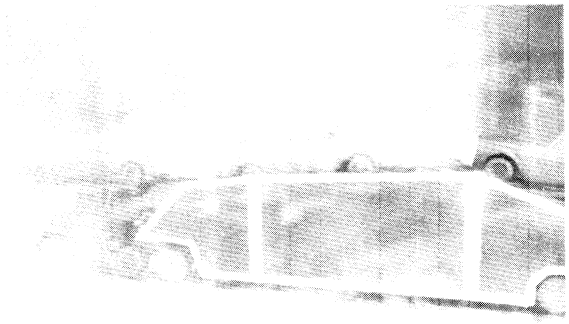

J

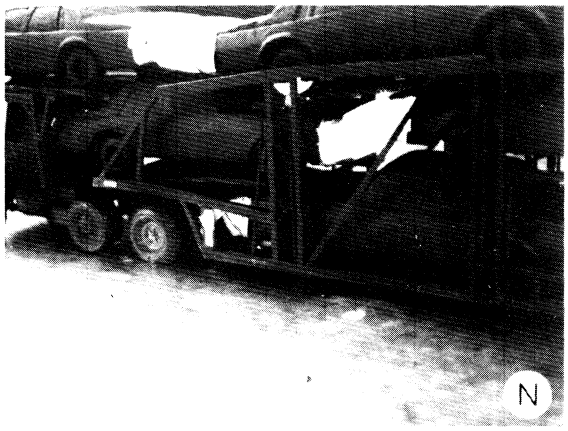

N

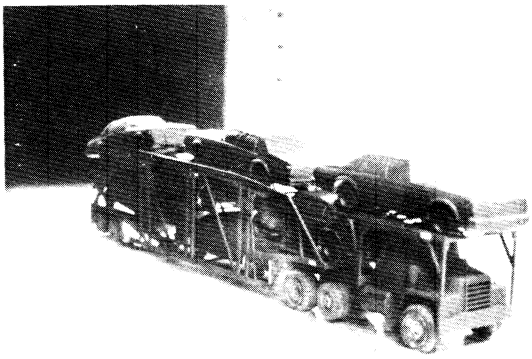

K

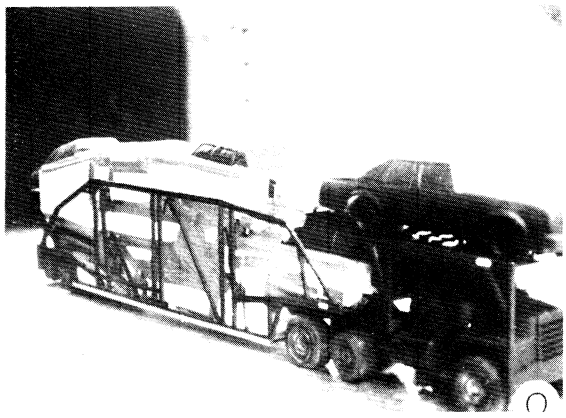

O

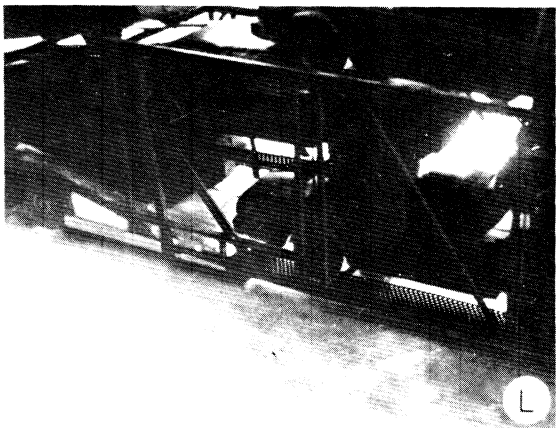

L

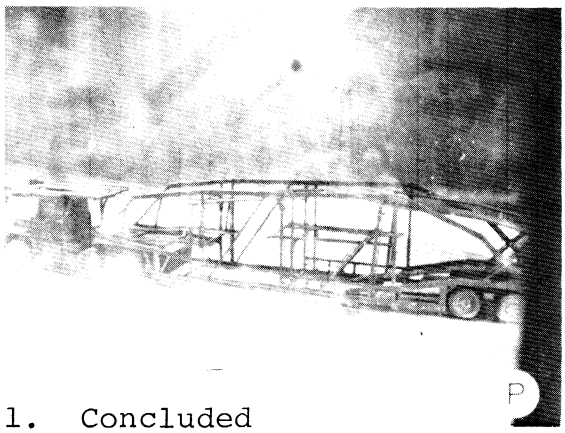

P

Figure B.1. Concluded

TABLE B-II CONFIGURATIONS TESTED - 65 FT UNIT

(Photographs are Shown in Fig. B-2)

Configuration No. 65-	
8-01 Baseline Photo A	The model of the 65 ft unit with the 8 cars having orientation number 1. Almost all tests were made with the 8 cars mounted in this configuration, as shown in Fig. B-II.
8-01 M1 Photo B	Full side panels on both sides of truck, both front and back units.
8-01 M1,CF Photo C	Full side panels plus a fairing between the cab and the sidewalls on the front unit.
8-01 M1,R No Photo	Full side panels on right side only. Note: In these wind tunnel tests the right side of the truck was always upwind whenever there was a crosswind (i.e. when ψ was greater than zero). Therefore, in considering the results of panels on one side only, the right side should be thought of as the upwind side and the left side thought of as the downwind side. Since the crosswind can be generally expected to come from either side, the overall benefits of adding panels on only one side can best be evaluated by using the average drag for these two (right and left panel) cases.
8-01 M1,R,RCF No Photo	Full side panels on right side plus a fairing between the cab and the right side panel on the front unit.
8-01 M1,L No Photo	Full side panels on left side only.
8-01 M1,L,LCF No Photo	Full side panels on left side plus a fairing between the cab and the left side panel on the front unit.
8-01 M1, Back No Photo	Side panels on both sides of the back unit; note that a small region (on both sides) near the back was not covered.
8-01 M1,R Back No Photo	Side panel on right side of back unit.
8-01 M1, L Back No Photo	Side panel on left side of back unit.
8-01 M1, Front No Photo	Panels on both sides of front unit.

TABLE B-II (Concluded)

Configuration No. 65-	
8-01 M1, R Front No Photo	Panel on right side of front unit.
8-01 M1, L Front No Photo	Panel on left side of front unit.
8-01 M1, Lower Photo D	Partial panels only, on all sides.
8-01 M1, Back Lower No Photo	Partial panels on back unit only.
8-01 M2 Photo E	Porous panels on all sides
8-01 M2 R No Photo	Porous panels on right side only.
8-01 M2, L No Photo	Porous panel on left side only.
8-01 M2, Front No Photo	Porous panels on both sides of front unit.
8-01 M3 Photo F	Baseline configuration except that a bottom panel was installed on the back unit.
8-02 Baseline Photo G	The position of certain cars near the front was changed.
Empty Baseline No Photo	Empty truckaway unit
Empty M1 No Photo	Panels on all sides of empty unit.

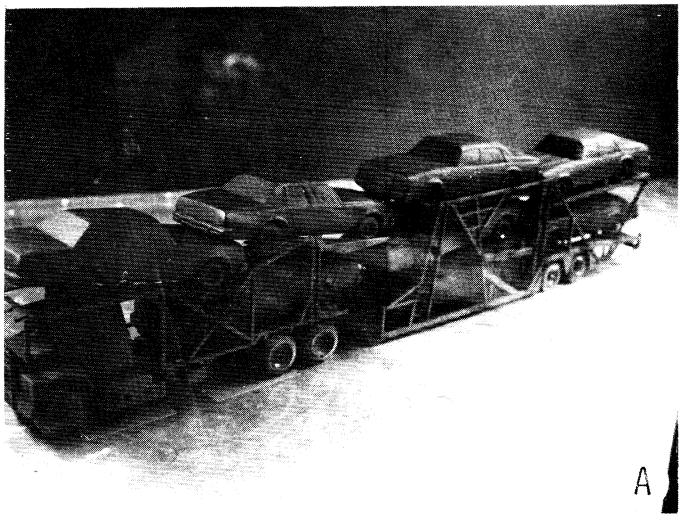

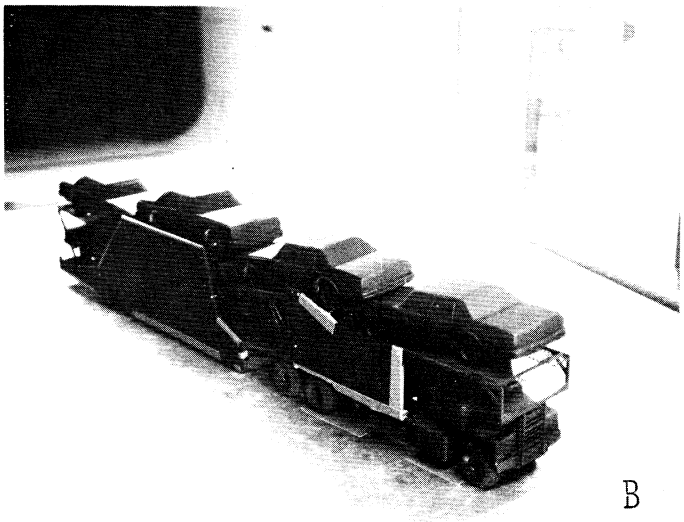

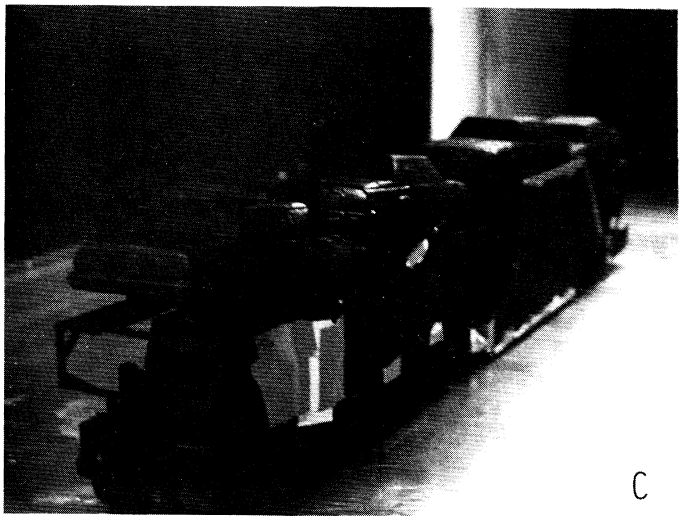

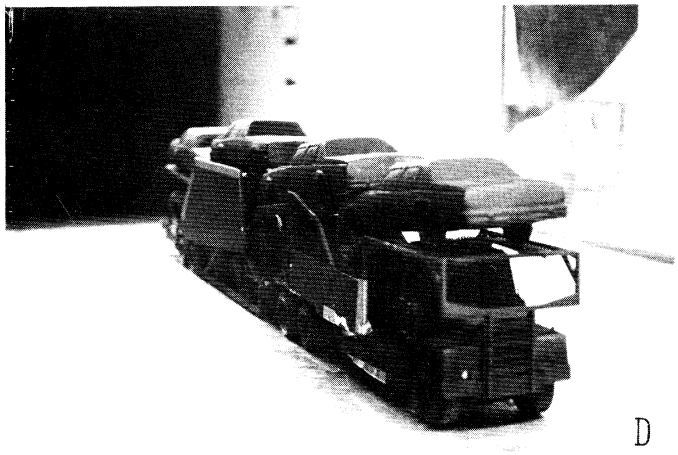

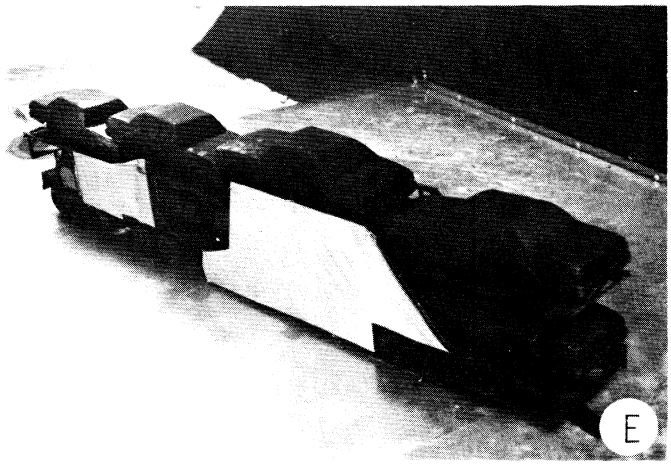

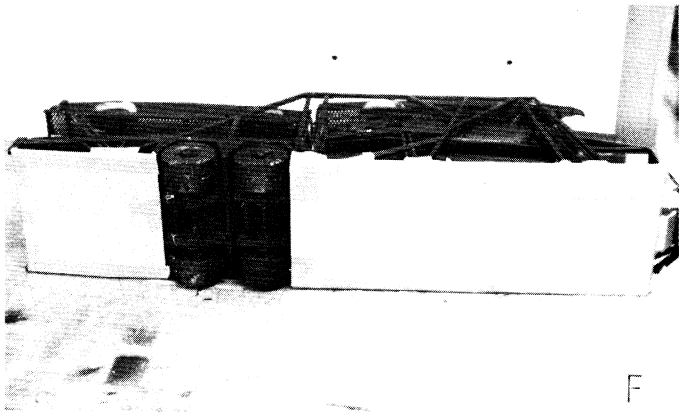

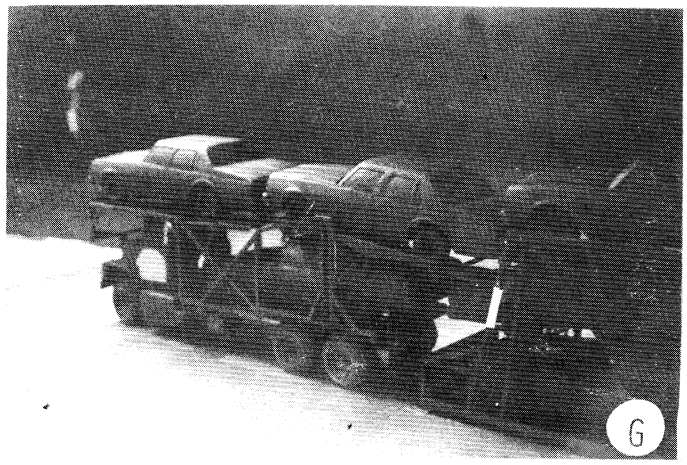

Figure B-2. Photographs of Model Configurations Tested
65 ft Unit

APPENDIX C
DETAILED TEST RESULTS

These wind tunnel tests of models of 55 ft and 65 ft truckaway units have produced drag data for a great many different configurations. In many cases the test results do not lend themselves to graphical presentation. Therefore, the test results are presented in tabular form; where practical, the results are also presented in graphical form.

The tables which follow have many "blanks" in them. This is due to the fact that it was not possible (in the time available) to test all of the configurations studied at all angles of yaw under consideration. Thus, while certain basic configurations were tested at yaw angles (ψ) of 0, 5, 10, 15 and 20°, some of the intermediate configurations were tested only at ψ = 20°. The 20° yaw angle was considered to be the most severe condition to be expected; any significant reductions in drag would be expected to show up at ψ = 20°.

These wind tunnel tests of 1/12 scale models of truckaway units were generally made at different air velocities in order to evaluate Reynolds number effects. There was <u>generally</u> a slight decrease in C_D with increasing Reynolds, as would be expected, but these changes were very slight; sometimes C_D increased slightly with Reynolds number. Therefore, the effects of Reynolds number variation have been ignored in the data presented.

At the lower velocities (e.g. below 55 mph) there was somewhat more scatter in the C_D data. Since the forces involved are all much smaller at low velocities, and thus the percentage error possible in the tunnel balance system readings is greater, it was concluded that the values of C_D measured at higher velocities would be used. Thus, most of the values of C_D listed in Tables C-I and C-II were obtained at tunnel air velocities of about 110 mph. As noted in Appendix A, the values of C_D can be used to determine the aerodynamic drag at any truck speed of interest.

In all cases the value of C_D listed is the average of at least three sets of measurements. In some cases more than one group of three sets were averaged.

The results of many preliminary tests of the 55 ft unit have not been included here. As a result of the early tests some of the test procedures were changed and the data obtained thereafter was more consistent. However, these earlier tests indicated the same trends and comparative results as did the tests covered by Tables C-I and C-II.

TABLE C-I TEST RESULTS FOR THE 55 FT UNIT

(Drag Coefficient, C_D, Listed in Body of Table.)

Configuration No. 55-	Photo No. in Fig. B-I	Yaw Angle, ψ					Percent Change in C_D
		0	5	10	15	20	ψ = 20
7-01 Baseline	A					1.75	+ 5.4
Loaded Conf. First Tested							
7-02 Baseline Second Conf. Tested	B					1.71	+ 3.0
7-03 Baseline Ref. Conf.	C	.81	.92	1.19	1.40	1.66	0 (Ref.)
7-03 M1 Bottom Panel Added	none					1.69	+ 1.8
7-03 M2 "Extended" Front Bumper	D[1]					1.72	+ 3.6
7-03 M3A Partial Side Panels, Both Sides	E					1.26	- 24.1
7-03 M4 Full Side Panels, Both Sides	F[2]	.79				1.19	- 28.3
7-03 M4 + M1 Bottom Panel Added to Full Side Panels	none					1.17	- 29.5
7-03 M4R Panels on Right (Upwind) Side	G					1.20	- 27.7

[1]Photo D is of Configuration 7-01 M2 since a photograph of 7-03 M2 was not taken. The extended bumper configuration was the same for both cases. The data listed is for 55-7-03 M2, as noted.

[2]Photo F shows side panels on truck model with cars in Orientation No. 1; picture of panels with Orientation No. 3 not available.

TABLE C-I (continued)

Configuration No. 55-	Photo No. in Fig. B-I	Yaw Angle, ψ					Percent Change in C_D $\psi = 20$
		0	5	10	15	20	
7-03 M4R + M1 Panels on Right Plus Bottom Panel	none					1.23	- 25.9
7-03 M4L Panels on Left Side	none					1.40	- 15.7
7-03 M4L-M1 Panels on Left Side Plus Bottom Panel	none					1.35	- 18.7
7-03 M5 Trailer Front Bulkhead Removed	none					1.64	- 1.2
7-01 M6 Fairing Behind Cab	H					1.80	+ 8.4
7-03 M7 Foam Between Cars	I					1.57	- 5.4
7-03 M4L + M7 Left Panel Plus Foam Between Cars	J					1.35	- 18.7
7-03 M4L + M7A Variation on 7-03 M4L + M7	none					1.37	- 17.5
7-03 M7B Foam Between Bottom Cars	none					1.59	- 4.2

TABLE C-I (concluded)

Configuration No. 55-	Photo No. in Fig. B-I	Yaw Angle, ψ					Percent Change in C_D ψ = 20
		0	5	10	15	20	
7-03 M7C Insert at Bottom Rear of Trailer	K					1.62	- 2.4
7-03 M7D Smoother Insert Than M7C	L					1.62	- 2.4
7-03 M7E Foam Between Cars and at Back of Trailer	M					1.54	- 7.2
7-03 M7F Variation on 7-03 M7E	N					1.53	- 7.8
7-03 M7F + M3R Fill in Between Car and Right (upwind) Side of Cars "Covered"	O	.75		.93		1.24	- 25.3
7-03 M7F + M3R + M1 Bottom Panel Added to Above	none	.74		.92		1.17	- 29.5
Empty - Baseline	P	.65	.752	.94	1.11	1.27	- 23.5

TABLE C-II TEST RESULTS FOR THE 65 FT UNIT

(Drag Coefficient, C_D, Listed in Body of Table.)

Configuration No. 65-	Photo No. in Fig. B-II	Yaw Angle, ψ					Percent Change in C_D
		0	5	10	15	20	ψ = 20
8-01 Baseline	A	.87	.95	1.26	1.57	1.80	0 (Ref.)
8-01 M1 Full Side Panels	B	.78	.83	1.05	1.28	1.48	- 17.8
8-01 M1, CF Side Panels and Cab Fairing	C	.77		.96		1.39	- 22.8
8-01 M1,R Right, Upwind, Side Panel	none	.81	.89	1.14	1.35	1.48	- 17.8
8-01 M1,R,RCF Right Side Panel and Cab Fairing	none	.80				1.40	- 22.2
8-01 M1,L Left, Downwind, Side Panel	none	.83	.88	1.15	1.42	1.64	- 8.9
8-01 M1,L,LCF Left Side Panel and Cab Fairing	none	.84				1.49	- 17.2
8-01 M1, Back Main Panels on Back Unit (Both Sides)	none					1.61	- 10.5
8-01 M1, R Back Main Panel on Right of Back Unit	none					1.60	- 11.1
8-01 M1, L Back Main Panel on Left of Back Unit	none					1.72	- 4.4

TABLE C-II (continued)

Configuration No. 65-	Photo No. in Fig. B-II	Yaw Angle, ψ					Percent Change in C_D
		0	5	10	15	20	ψ = 20
8-01 M1, Front Panels on Front Unit (Both Sides)	none					1.70	- 5.6
8-01 M1,R Front Panel on Right of Front Unit	none					1.72	- 4.4
8-01 M1, L Front Panel on Left of Front Unit	none					1.76	- 2.2
8-01 M1, Partial Partial Panels All Sides	D	.82				1.62	- 10.0
8-01 M1, Partial, Back Partial Panels, Back Unit	none	.83				1.64	- 8.9
8-01 M2 Porous Side Panels	E					1.69	- 6.1
8-01 M2,R Porous Panels on Right Side	none					1.66	- 7.8
8-01 M2,L Porous Panels on Left Side	none					1.81	+ 0.6
8-01 M2, Front Porous Panels on Front Unit	none					1.73	- 3.9

TABLE C-II (concluded)

Configuration No. 65-	Photo No. in Fig. B-II	Yaw Angle, ψ					Percent Change in C_D ψ = 20
		0	5	10	15	20	
8-01 M3 Bottom Panel Only	F	.863				1.74	- 3.3
8-02 Baseline Change in Orientation of Some Cars	G	.868				1.76	- 2.2
Empty - Baseline Empty Truck	none	.696				1.38	- 23.3
Empty M1 Panels on All Sides	none	.601				1.16	- 35.6

APPENDIX D

DESCRIPTION OF THE UNIVERSITY OF MICHIGAN'S LOW TURBULENCE WIND TUNNEL

Gas Dynamics Laboatories
Department of Aerospace Engineering

The subsonic tunnel in this facility is a closed circuit, single return tunnel with an essentially rectangular test section 7 ft wide by 5 ft high by 25 ft long. (The corners of the test section are filleted 8 in. up each wall, thus reducing the cross-sectional area to about 34 ft^2.) Several fine mesh screens in the settling chamber combined with the high contraction ratio (15:1) result in unusually low turbulence in the test section.

The tunnel is capable of continuous operation at test section velocities of up to 130 knots (150 mph) with a model having an effective blockage of about 3 ft^2. Somewhat higher velocities are attainable with less blockage.

The front side of the tunnel has many windows in it and a few windows are in the top of the tunnel. The side windows, especially, provide relatively good opportunity for viewing or photographing the model. Additional windows could be provided where specifically needed.

The wind tunnel facilities have instrumentation systems for the measurement and recording of all necessary quantities. Pressure measurements are made by a variety of manometers and pressure transducers. A Scanivalve system is available which is set up to rapidly record in sequence up to 48 separate pressures. A data acquisition system controls the operation of the Scanivalve unit and records the output of the pressure transducer mounted in the Scanivalve. The output of the transducer

is digitized to an accuracy of better than 0.1% of full scale. This digitized output is in the form of punched paper tape which in turn can be read into the Laboratories' computer for data reduction. Both printouts of the results and appropriate graphs can be provided by this computer system (a NOVA 840). Alternatively, the results would be read into the University's time sharing system (MTS, which includes an AMDAHL 470 V/6 Computer) for data reduction and output of results. The results could also be fed to the Laboratories' "Computer Graphics" facilities in a variety of graphical forms for visual inspection. The tape could also be fed into a Teletype connected to a telephone line for remote handling of the test results.

The force and moment data for a model being tested are obtained from the wind tunnel balance system. This balance is mounted below the tunnel test section with the support post (3.0 in. in diameter) passing through the tunnel floor for attachment to the model. (A flange joint in this post at the floor level allows different "units" to be easily mounted within the tunnel and still be supported by the external balance system.) A hollow support post is used to facilitate the routing of flexible tubing from the model pressure taps to the pressure measuring system. This balance system can support models having gross weights of over 300 lbs. It provides for the measurement of all 3 force components and all 3 moment components by means of various combinations of strain gauges.

The ranges of the six components are as follows:

Lift Force	600 lb	Pitch Moment	3,000 in. lb
Drag Force	120 lb	Roll Moment	3,000 in. lb
Side Force	80 lb	Yaw Moment	1,800 in. lb

Accuracies of one part in 3,000 are attainable with this balance. Interaction errors are on the order of .1%.

The six strain gauge signals, corresponding to each of the six force and moment components, are fed into variable gain amplifiers and the outputs are displayed by digital panel voltmeters. The tunnel dynamic pressure and temperature as well as

the date, time and certain other variables are also displayed on digital panel meters. All these displayed values can be recorded manually if desired, but all the meters are also equipped to output to a data acquisition system. With this system, simultaneous readings of all meters are recorded on paper tape whenever a record of test data is desired. The paper tape can then be fed into a computer to provide a print-out or graph of the desired parameters, or otherwise handled as noted earlier for the tapes of the pressure measurement data. (If necessary, the data acquisition systems could be tied directly to a telephone line for instantaneous transmission of the test results.)

Boundary layer velocity profiles on the tunnel walls or on the model can be obtained via a hot wire probe translated through the boundary layer. Probes will either be supported from the model proper with an internal support-translation mechanism or through the wind tunnel wall with the support-translation outside the tunnel. Final choice of support depends on both model design and the locations on the model where boundary layer velocity profiles are required. Both hot wire and hot film "Disa" instrumentation systems are available for these measurements.

The Laboratories have extensive facilities for flow visualization. A number of flow tracing techniques have been used in this facility. These include tufts on the model surface, the introduction of helium filled bubbles or smoke into the flow, small vanes mounted on a given surface to show flow direction, coating the model with oil, etc. A number of photographic systems are available for recording this type of data. Photographic systems from a simple Polaroid camera through motion picture cameras (5 frames/sec through 1 million frames/sec) are available for these purposes.

Special facilities have been developed to enable various models to be tested in a boundary layer simulating the earth's boundary layer. These facilities include a turntable, 5 ft in diameter, on which the building models can be mounted. In this way the flow patterns over and around the model can be studied for any wind direction. Any of the various flow tracing techniques mentioned earlier may be used to indicate the flow pattern around the model. Procedures have been developed to artificially thicken the boundary layer above the tunnel floor in order to simulate the appropriate type of boundary layer (e.g. flat prairie, rural/urban, or inner city) for the particular model being tested.

A ground plane system has also been designed and built for testing models of various automotive type vehicles, which need to be tested while mounted close to a surface that has a negligible boundary layer. The ground plane is mounted above the tunnel floor outside of the tunnel boundary layer. The turntable in this ground plane system is 5 ft in diameter. Models are supported by the balance system so that they are positioned just above the ground plane surface, without touching the ground plane.

THE UNIVERSITY OF MICHIGAN

DATE DUE

3/21 5:46 PM	
12/18 9:00P	